AD-A103 421 KR+ LASER EXCITATION OF NH2 IN ATMOSPHERIC PRESSURE FLAMES(U) ARMY BALLISTIC RESEARCH LAB ABERDEEN PROVING GROUND MD W R ANDERSON ET AL. 13 APR 87 BRL-TR-2805 1/1

UNCLASSIFIED F/G 7/2 NL

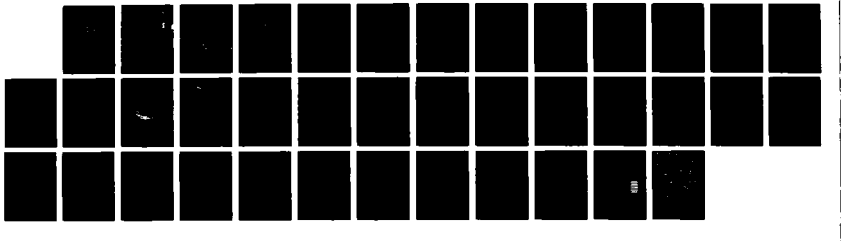

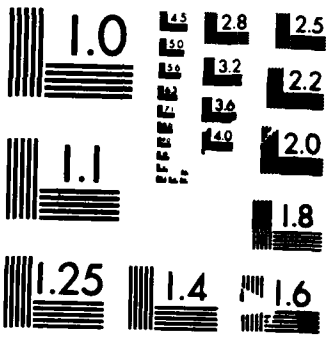

MICROCOPY RESOLUTION TEST CHART
NATIONAL BUREAU OF STANDARDS-1963-A

TECHNICAL REPORT BRL-TR-2805

KR+ LASER EXCITATION OF NH2 IN ATMOSPHERIC PRESSURE FLAMES

WILLIAM R. ANDERSON, JOHN A. VANDERHOFF
ANTHONY J. KOTLAR, KOON N. WONG

APRIL 13, 1987

US ARMY BALLISTIC RESEARCH LABORATORY
ABERDEEN PROVING GROUND, MARYLAND

UNCLASSIFIED
SECURITY CLASSIFICATION OF THIS PAGE

ADA 183 421

REPORT DOCUMENTATION PAGE

Form Approved
OMB No 0704-0188
Exp. Date Jun 30, 1986

1a. REPORT SECURITY CLASSIFICATION Unclassified	1b. RESTRICTIVE MARKINGS
2a. SECURITY CLASSIFICATION AUTHORITY	3. DISTRIBUTION/AVAILABILITY OF REPORT
2b. DECLASSIFICATION/DOWNGRADING SCHEDULE	
4. PERFORMING ORGANIZATION REPORT NUMBER(S)	5. MONITORING ORGANIZATION REPORT NUMBER(S)
6a. NAME OF PERFORMING ORGANIZATION US Army Ballistic Research Laboratory 6b. OFFICE SYMBOL (If applicable) SLCBR-IB	7a. NAME OF MONITORING ORGANIZATION
6c. ADDRESS (City, State, and ZIP Code) Aberdeen Proving Ground, MD 21005-5066	7b. ADDRESS (City, State, and ZIP Code)
8a. NAME OF FUNDING/SPONSORING ORGANIZATION 8b. OFFICE SYMBOL (If applicable)	9. PROCUREMENT INSTRUMENT IDENTIFICATION NUMBER
8c. ADDRESS (City, State, and ZIP Code)	10. SOURCE OF FUNDING NUMBERS PROGRAM ELEMENT NO. 61102A; PROJECT NO. AH43; TASK NO.; WORK UNIT ACCESSION NO

11. TITLE (Include Security Classification)

Kr^+ Laser Excitation of NH_2 in Atmospheric Pressure Flames

12. PERSONAL AUTHOR(S)
K.N. Wong,* W.R. Anderson, J.A. Vanderhoff, and A.J. Kotlar

13a. TYPE OF REPORT	13b. TIME COVERED	14. DATE OF REPORT (Year, Month, Day)	15. PAGE COUNT
Final	FROM Jan 84 TO Oct 85		

16. SUPPLEMENTARY NOTATION
*NRC Postdoctoral Research Associate.
Published in Journal of Chemical Physics

17. COSATI CODES		
FIELD	GROUP	SUB-GROUP
07	04	
21	02	

18. SUBJECT TERMS (Continue on reverse if necessary and identify by block number)
Laser Induced Fluorescence, Combustion, NH_2 Radical, Ammonia, Methane, Absolute Intensities, NH_3/N_2O Flame, CH_4/N_2O Flame, Nitrous Oxide, Hydrogen, H_2/N_2O Flame

19. ABSTRACT (Continue on reverse if necessary and identify by block number)

Fluorescence in the A-X system of the NH_2 radical has been excited in $NH_3/N_2O/N_2$, $H_2/N_2O/N_2$ and $CH_4/N_2O/N_2$ flames using the 6471Å line of a krypton ion laser. Trace species in the $H_2/N_2O/N_2$ flame are of interest because reactions which take place in this flame are expected to be a subset of the gas phase reactions in the combustion of propellants. Detection of NH_2 fluorescence was found to be very simple to implement using the krypton laser. Rotationally resolved fluorescence spectra indicate that the laser simultaneously pumps two rotational lines in the (0,11,0)-(0,2,0) vibrational hot band of the radical. The placement of the laser line relative to the two molecular transitions has been inferred from intensities in the fluorescence spectrum. Rotational and vibrational energy transfer in the excited state were observed to be very slow in comparison to electronic quenching by the flame molecules. An NH_2 density profile in a rich $H_2/N_2O/N_2$ flame is given. Also, a method for the calculation of Einstein coefficients and oscillator strengths for nonperturbed, main-branch transitions is presented.

20. DISTRIBUTION/AVAILABILITY OF ABSTRACT	21. ABSTRACT SECURITY CLASSIFICATION
☐ UNCLASSIFIED/UNLIMITED ☒ SAME AS RPT. ☐ DTIC USERS	Unclassified

22a. NAME OF RESPONSIBLE INDIVIDUAL	22b. TELEPHONE (Include Area Code)	22c. OFFICE SYMBOL
DR. WILLIAM R. ANDERSON	301-278-7070	SLCBR-IB-I

DD FORM 1473, 84 MAR — 83 APR edition may be used until exhausted. All other editions are obsolete.

SECURITY CLASSIFICATION OF THIS PAGE

UNCLASSIFIED

INSTRUCTIONS FOR PREPARATION OF REPORT DOCUMENTATION PAGE

GENERAL INFORMATION

The accuracy and completeness of all information provided in the DD Form 1473, especially classification and distribution limitation markings, are the responsibility of the authoring or monitoring DoD activity.

Because the data input on this form will be what others will retrieve from DTIC's bibliographic data base or may determine how the document can be accessed by future users, care should be taken to have the form completed by knowledgeable personnel. For better communication and to facilitate more complete and accurate input from the originators of the form to those processing the data, space has been provided in Block 22 for the name, telephone number, and office symbol of the DoD person responsible for the input cited on the form.

All information on the DD Form 1473 should be typed.

Only information appearing on or in the report, or applying specifically to the report in hand, should be reported. If there is any doubt, the block should be left blank.

Some of the information on the forms (e.g., title, abstract) will be machine indexed. The terminology used should describe the content of the report or identify it as precisely as possible for future identification and retrieval.

NOTE: **Unclassified abstracts and titles describing classified documents may appear separately from the documents in an unclassified context, e.g., in DTIC announcement bulletins and bibliographies. This must be considered in the preparation and marking of unclassified abstracts and titles.**

The Defense Technical Information Center (DTIC) is ready to offer assistance to anyone who needs and requests it. Call Data Base Input Division, Autovon 284-7044 or Commercial (202) 274-7044.

SECURITY CLASSIFICATION OF THE FORM

In accordance with DoD 5200.1-R, Information Security Program Regulation, Chapter IV Section 2, paragraph 4-200, classification markings are to be stamped, printed, or written at the top and bottom of the form in capital letters that are larger than those used in the text of the document. See also DoD 5220.22-M, Industrial Security Manual for Safeguarding Classified Information, Section II, paragraph 11a(2). This form should be unclassified, if possible.

SPECIFIC BLOCKS

Block 1a. Report Security Classification: Designate the highest security classification of the report. (See DoD 5220.1-R, Chapters I, IV, VII, XI, Appendix A.)

Block 1b. Restricted Marking: Enter the restricted marking or warning notice of the report (e.g., CNWDI, RD, NATO).

Block 2a. Security Classification Authority: Enter the commonly used markings in accordance with DoD 5200.1-R, Chapter IV, Section 4, paragraph 4-400 and 4-402. Indicate classification authority.

Block 2b. Declassification / Downgrading Schedule: Indicate specific date or event for declassification or the notation, "Originating Agency Determination Required" or "OADR." Also insert (when applicable) downgrade to _____ on _____ (e.g., Downgrade to Confidential on 6 July 1983). (See also DoD 5220.22-M, Industrial Security Manual for Safeguarding Classified Information, Appendix II.)

NOTE: **Entry must be made in Blocks 2a and 2b except when the original report is unclassified and has never been upgraded.**

Block 3. Distribution/Availability Statement of Report: Insert the statement as it appears on the report. If a limited distribution statement is used, the reason must be one of those given by DoD Directive 5200.20, Distribution Statements on Technical Documents, as supplemented by the 18 OCT 1983 SECDEF Memo, "Control of Unclassified Technology with Military Application." The Distribution Statement should provide for the broadest distribution possible within limits of security and controlling office limitations.

Block 4. *Performing Organization Report Number(s)*: Enter the unique alphanumeric report number(s) assigned by the organization originating or generating the report from its research and whose name appears in Block 6. These numbers should be in accordance with ANSI STD 239.23-74, "American National Standard Technical Report Number." If the Performing Organization is also the Monitoring Agency, enter the report number in Block 4.

Block 5. Monitoring Organization Report Number(s): Enter the unique alphanumeric report number(s) assigned by the Monitoring Agency. This should be a number assigned by a DoD or other government agency and should be in accordance with ANSI STD 239.23-74. If the Monitoring Agency is the same as the Performing Organization, enter the report number in Block 4 and leave Block 5 blank.

Block 6a. Name of Performing Organization: For in-house reports, enter the name of the performing activity. For reports prepared under contract or grant, enter the contractor or the grantee who generated the report and identify the appropriate corporate division, school, laboratory, etc., of the author.

Block 6b. Office Symbol: Enter the office symbol of the *Performing Organization*.

Block 6c. Address: Enter the address of the Performing Organization. List city, state, and ZIP code.

Block 7a. Name of Monitoring Organization: This is the agency responsible for administering or monitoring a project, contract, or grant. If the monitor is also the Performing Organization, leave Block 7a blank. In the case of joint sponsorship, the Monitoring Organization is determined by advance agreement. It can be either an office, a group, or a committee representing more than one activity, service, or agency.

Block 7b. Address: Enter the address of the Monitoring Organization. Include city, state, and ZIP code.

Block 8a. Name of Funding/Sponsoring Organization. Enter the full official name of the organization under whose immediate funding the document was generated, whether the work was done in-house or by contract. If the Monitoring Organization is the same as the Funding Organization, leave 8a blank.

Block 8b. Office Symbol. Enter the office symbol of the Funding/Sponsoring Organization.

Block 8c. Address. Enter the address of the Funding/Sponsoring Organization. Include city, state and ZIP code.

TABLE OF CONTENTS

LIST OF FIGURES

I. INTRODUCTION

The amidogen (NH_2) radical has been a subject of extensive experimental and theoretical investigations since the discovery of its emission spectrum more than a century ago.[1] The two electronic states involved in the visible transition, $\tilde{A}^2A_1$ and $\tilde{X}^2B_1$, result from the Renner-Teller interaction;[2] that is, these two electronic states correlate with the doubly degenerate $^2\Pi$ state of the molecule in its linear configuration. Because the molecule is bent the π degeneracy is lifted, giving rise to the widely separated states $^2A_1$ and $^2B_1$ of C_{2v} symmetry. The ground state $^2B_1$ is bent with an equilibrium bond angle of ~103° and the upper state $^2A_1$ is quasi-linear with a bond angle of about 145°.[3] Aside from the interest in effects of the Renner-Teller interaction on the molecular structure, there is a great deal of interest in NH_2 because it plays an important role in atmospheric and combustion chemistry.[4-6] NH_2 is also believed to play a central role in the "thermal de-NO_x" process[7-9] wherein NH_3 is added to combustion effluents to remove NO from exhaust gases.

The absorption spectrum of NH_2 was first observed in the wavelength region 3900-8300Å during the flash photolysis of ammonia[10] and hydrazine.[11] Dressler and Ramsay[2] later performed a detailed rotational and vibrational analysis of the absorption spectra of NH_2 and ND_2 arising from the $\tilde{A}$-$\tilde{X}$ transition in this region. Johns, Ramsay and Ross[12] have extended the analysis to the long wavelength end of the spectrum and have identified all the low-lying bending vibronic levels of the excited state up to $v_2'=8$. Because of the complexity of the emission spectrum, no detailed analysis has been performed. Laser induced fluorescence (LIF) has been used to simplify the complex emission spectrum. In 1975, Kroll[13] used this technique to obtain approximate molecular constants for the (0,0,0), (0,1,0), (0,2,0), (1,0,0), (1,1,0), and (0,4,0) vibrational levels of the ground state. In addition, collisional dynamics of the excited state were studied. Vervloet and Merienne-Lafore[14] and Vervloet, Merienne-Lafore and Ramsay[15] also used LIF to aid in the analysis of the complex emission spectrum. LIF has also been used for the measurement of radiative lifetimes of several of the excited state vibrational levels.[16-18] Xiang, et al.,[19] have used LIF on NH_2 to study its reaction with NO_2 and vibrational deactivation by CH_3NH_2 and NH_3. Besides these techniques, NH_2 has been studied by infrared matrix isolation spectroscopy,[20] microwave-optical double resonance,[21] difference frequency laser spectroscopy,[22] infrared-optical double resonance[23] and coherent antistokes Raman spectroscopy.[24] Combined analyses of all the available data from the optical to the microwave region has resulted in very accurate molecular parameters.[25,26]

As mentioned previously, LIF is useful in that it simplifies the analysis of the complex emission spectrum. This technique is also a very powerful method for the detection of trace species in combustion systems because of its high sensitivity and selectivity.[27] Usually, tunable dye lasers have been used to excite the fluorescence. However, in recent work in this laboratory it has been shown that a number of radicals can be detected by LIF using the convenient and simpler Ar^+ or Kr^+ ion lasers. In addition, Raman spectroscopy can be used simultaneously to obtain majority species concentration and temperature.[28] Coincidences of the ion laser lines with molecular transitions have been discovered and used to study LIF of C_2 and CN,[29] NCO,[30] and OH and NH[28] in N_2O supported flames. NH_2 has previously been detected in ammonia

flames both by absorption[31,32] and by LIF[33] using tunable dye laser sources. In this paper, we report the excitation of NH_2 fluorescence using the 6471Å line of a Kr^+ laser. The radical is present in all N_2O supported flames which we have studied, namely flames of H_2, CH_4, and NH_3. Not surprisingly, the LIF intensities indicate the concentration of NH_2 is highest in the ammonia flame. These flames are of interest because N_2O is currently believed to be of importance in the combustion of nitramine and double base propellants.[34,35] The H_2 flame is of most interest in this regard because all of the hydrogen reactions in this flame are expected to occur in combustion of the propellants, whereas reactions of CH_4 and NH_3 are probably not significant. This paper will center around two major issues. First, the identification of the pump transition is obtained using spectra from the NH_3 flame. The second issue is the determination of NH_2 density in a flame from the fluorescence signal obtained using the ion laser. For purposes of demonstration, an accurate relative density profile through the reaction zone of a rich $H_2/N_2O/N_2$ flame and an estimate of the absolute NH_2 density in the flame will be presented. (Profiles for several other species in H_2/N_2O flames ranging from lean to stoichiometric mixture ratios are given in Ref. 28b).

II. EXPERIMENTAL

The experiment has been described in detail previously[30] and will only be briefly discussed here. Slightly rich premixed flames of fuel gases and nitrous oxide were supported on an open channel curved knife-edge burner.[36] The burner was placed at the intracavity focus of a krypton ion laser. Movement of this burner allows easy access to the entire flame zone. Since heat losses by the flame to this burner are small, the adiabatic flame temperature is generally reached. Radical concentrations for the burner are therefore, in general, higher than for other types of burner. This type of burner has thus been found to be extremely useful for spectroscopic studies of radicals, as well as determination of flame profiles, both in this laboratory and elsewhere.[33]

A nominal 3W (all lines) Kr^+ ion laser was used as the excitation source. The laser cavity was extended using two highly reflective mirrors with radii of curvature 1.0 and 0.3 m. The circulating intracavity laser power was about 50 watts. This power level is well below that required to observe effects of optical saturation, even with focusing. For the identification of the NH_2 pumping transition, the scattered light was focused onto the vertical slit of a 1 m monochromator. The monochromator was operated in the first order of a 1200 groove/mm grating blazed at 7500Å. Since the burner and laser beam have their long axes horizontal, a glass dove prism was placed in front of the slit to rotate the image 90°. The detected light comes from a volume approximately 100 microns in diameter and 3 mm in length. A silicon-intensified vidicon tube (OMA II) was used to detect the dispersed light. Approximately 50Å of the spectrum could be observed at one time with this system. The spectrum was recorded into 500 memory channels of the OMA II. The resolution was about 0.7Å. For the measurement of density and temperature profiles a 25 cm monochromator was used. Although the resolution of this system is lower, use of the smaller monochromator allows for the observation of about 400Å of the spectrum at a time. This larger observation range is useful because it allows simultaneous recording of the spontaneous Raman anti-Stokes signal from N_2 (used to monitor flame temperature) together

with the fluorescence from the strongest region of the NH_2 spectrum. A computer was used for data accumulation and processing. For a typical run, the LIF + flame emission spectrum was first obtained (laser on) and then a spectrum consisting only of the flame emission was obtained (laser off). The LIF spectrum was obtained by differencing these spectra. For the spectral investigations, an $NH_3/N_2O/N_2$ flame of equivalence ratio $\phi \approx 1.6$ was used. The dilution with N_2 was about 40%. For the measurement of density and temperature profiles in a $H_2/N_2O/N_2$ flame, the flows were measured with a wet test meter. The conditions were $\phi = 1.97$ with 44% dilution by N_2.

III. RESULTS AND DISCUSSION

A. Interpretation of the Fluorescence Spectra

Some general information regarding the $\tilde{A}$-$\tilde{X}$ transition of NH_2 may prove useful to this discussion. In the ground state, NH_2 is a bent, highly asymmetric top molecule; however, in high vibrational levels of the excited state, the molecule is quasi-linear and behaves like it has 2π symmetry.[2,3] Owing to the large change in the equilibrium bond angle in the two states, the absorption spectrum shows a long progression in the bending vibration, $\nu_2(a_1)$. Most of the features in the absorption spectrum arise from the main progression $(0,v_2',0)\leftarrow(0,0,0)$. The strongest bands are those at about $v_2'=9$. In addition, a subsidiary progression, $(1,v_2',0) \leftarrow (0,0,0)$, has also been observed. Dressler and Ramsay showed that the absorption spectrum consists of type C bands for which the rotational selection rules are $\Delta N=0, \pm1$, $\Delta K_a=\pm1, \pm3, \ldots$ and $\Delta K_c=0, \pm2, \ldots$ where N is the total angular momemtum excluding spin. The transition $\tilde{A}^2A_1 - \tilde{X}^2B_1$ is allowed by dipole selection rules. Therefore in this transition the non-totally symmetric vibration $\nu_3(b_2)$ must change by an even number of quanta, but the totally symmetric vibrations $\nu_1(a_1)$ and $\nu_2(a_1)$ can change by any number of quanta. Another important feature of the spectrum is that successive rotational lines show an alternation in the intensities because of the nuclear spin symmetry properties of NH_2. Since the H nuclei have spin 1/2, the line intensities show a 1:3 alternation similar to that observed for H_2.[37]

In the excited state, K_a' is a good quantum number given by the vector sum of the orbital angular momentum and the vibrational angular momentum, i.e., $K_a' = |\pm\Lambda \pm \ell|$. In this case $\Lambda=1$, since the state correlates to a $^2\pi$ state, and ℓ is given by v', v'-2, v'-4, ..., 1 or 0 depending on whether v' is even or odd. Thus, for odd v', $K_a'=0, 2, 4, \ldots, v'-1$ and, for even v', $K_a'=1, 3, 5, \ldots, v'-1$. ($K_a' = v'+1$ levels are not observed in the excited state because, as demonstrated in Ref. 2, these levels from the "original" $^2\pi$ state of linear NH_2 correlate to levels in the $\tilde{X}^2B_1$ state when the molecule becomes bent.) Large vibronic splittings of the K_a' levels are observed due to the Renner-Teller effect. The bands with $K_a'=0, 1, 2, 3, 4, \ldots$ are referred to as Σ, π, Δ, Φ, Γ, ... vibronic subbands, respectively. In the following, we will show that the 6471Å line of the krypton ion laser pumps to the $(0,11,0)\Sigma$ vibronic level of the excited state.

Several years ago in this laboratory, low resolution Raman spectra (~4A FWHM) of majority species in $CH_4/N_2O/N_2$ flames were being studied.[38] During the course of these studies, an intense, unidentified fluorescence spectrum was observed in the region of 5430Å using the 6471Å line of the

krypton ion laser.[39] Under low resolution, the spectrum appears to consist of a simple P and R branch structure. Therefore, it was originally thought that the fluorescence might be due to a $\Delta\Lambda=0$ transition of some linear molecule. More recently, however, spectra have been taken at higher resolution using the 1 m monochromator. The higher resolution spectrum in the 5430Å region is much more complicated than originally believed. It consists of a series of lines of highly irregular intensities (see Figure 1) whose interpretation was not immediately obvious. In addition, the sensitivity was increased by averaging up to ~1000 OMA scans. It was thus found that, although the 5430Å region contains the most intense fluorescence (uncorrected for detector system response), the spectrum extends to at least 8050Å. It should be noted that the region of the laser line was not scanned because of intense interference from laser scatter. Also, at wavelengths longer than 8000Å the OMA sensitivity becomes too small to allow detection of all but the strongest signals.

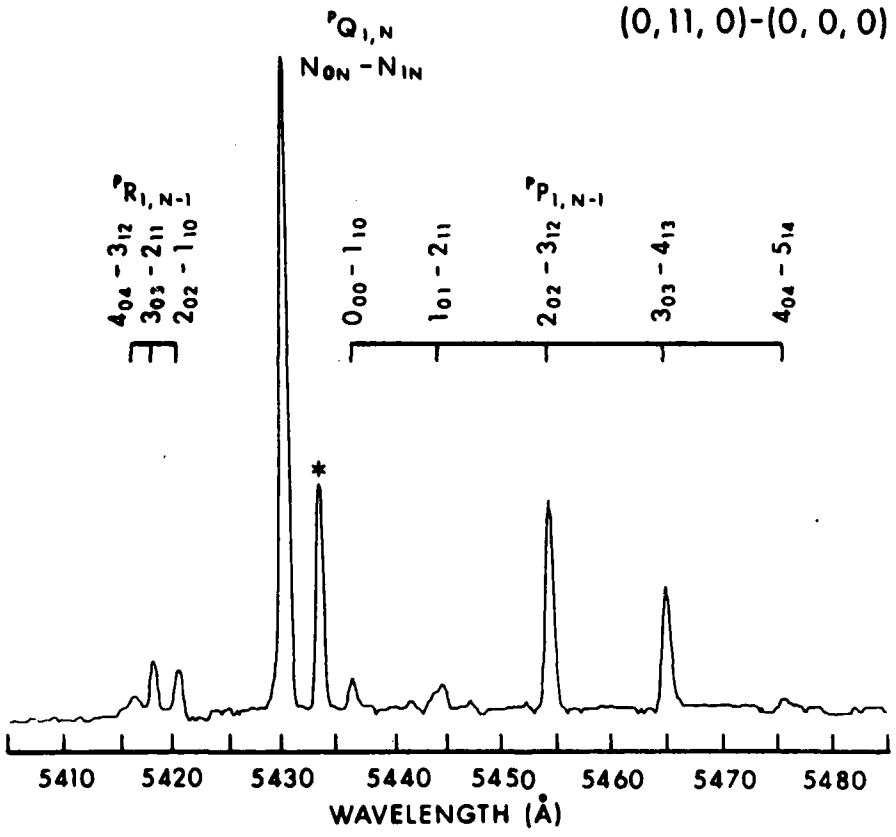

Figure 1. The (0,11,0)-(0,0,0)Σ band of the $\tilde{A}$-$\tilde{X}$ transition of NH_2. The fluorescence was excited using the 6471Å line of a Kr^+ laser. The line indicated by * is unidentified.

At first, it was not known for certain that NH_2 was responsible for the observed spectrum. A preliminary attempt to search the entire spectrum for patterns of lines similar to that in the 5430Å region, thus helping to

identify vibrational spacings, failed. Definite evidence that the spectrum arises from NH_2 was obtained from the observation of some easily recognized Q heads of the $^2A_1$-$^2B_1$ transition in both the flame emission and LIF spectra. They occur at 5708Å [(0,10,0)], 5977Å [(0,9,0)], 6302Å [(0,8,0)], and 6620Å [(0,7,0)]. (Here the notation refers to the excited state vibrational level. This notation is intended to indicate that (0,0,0) is the ground state level.) Thereafter, efforts were concentrated upon the task of assigning the pumping transition and, especially, the intense features in the 5430Å region. The key to the assignment was in making the assumption that the 6471Å laser line pumps a vibrational hot band whose excited state then emits to the (0,0,0) level of $\tilde{X}^2B_1$. The shortest wavelength fluorescence of appreciable intensity, i.e., that of the 5430Å region, would thus be ascribable to the laser excited state. Upon comparison of the line positions with those in Ref. 2, it was found that all but one of the lines in this region coincide with rotational transitions of the (0,11,0)-(0,0,0)Σ vibronic subband of NH_2, thus firmly identifying the emitter. The assignments of the lines are given in Figure 1. This band is rather simple in comparison to others for two reasons.[2] First, since it is a Σ subband, it consists of only three strong branches, $^PP_{1,N-1}$, $^PQ_{1,N}$, and $^PR_{1,N-1}$.* Second, spin splitting of lines in this subband is so small that only single lines are observed, even at a resolution of a few tenths of a cm^{-1}.

Upon first inspection of Figure 1, it appears that 2_{02} may be the only upper state rotational level pumped by the laser because the 2_{02}-3_{12} transition is much more intense than others in the $^PP_{1,N-1}$ branch. Collisionally induced rotational energy transfer would then give rise to the other less intense peaks. However, if both the 1_{01} and 3_{03} states are populated solely by rotational energy transfer, it is difficult to explain the much higher intensity of the 3_{03}-4_{13} as compared to the 1_{01}-2_{11} transition. In addition, 1_{01} and 3_{03} are ortho levels while 2_{02} is a para level. Kroll[13] and Halpern, et al.,[16] have shown that energy transfer between ortho and para states is extremely slow, much as it is for H_2. These observations suggest that both the 2_{02} and 3_{03} excited state levels are being pumped simultaneously by the 6471Å laser line. This conclusion is supported by the following calculations. It is a simple matter to determine that the 6471Å line is in the region of the (0,11,0)-(0,2,0)Σ vibronic transition. Table 1 shows calculations of some rotational transitions of this band. (These transitions were calculated in the following manner. Excited state term values were obtained by adding the appropriate ground state term values to the transition frequencies of the (0,11,0)-(0,0,0)Σ band of Ref. 2. Overlapped lines from Ref. 2 were not used. In this note, term values calculated in this way will be referred to as "measured" term values. These "measured" term values were fitted to the equation $F = T_o + BN(N+1) - DN^2(N+1)^2 + HN^3(N+1)^3$ to check for possible deviations. The "measured" term value calculated using the 2_{02}-1_{10} transition was rejected since it differed significantly from the fitted value. Multiple determinations of the same excited state "measured" term value were then averaged. The unobserved (0,11,0)-(0,2,0)Σ transitions were calculated from the appropriate (0,2,0) value and from these averaged

*Here, the notation follows that of Ref. 2 and refers to $^{\Delta K_a}\Delta N_{K_a"K_c"}$.

upper state term values, without spin-splitting, were calculated using the constants of Ref. 26. Note that for the excited vibrational level, four parameters in the term value equation are fitted. The remaining higher order centrifugal distortion constants are not well determined. In Ref. 2 only the first three terms were used. For the $(0,11,0)\Sigma_1$ level we found: T_o = 18430.195 ± 0.026 cm^{-1}, B = 8.9686 ± 0.0047 cm^{-1}, D = -8.08 ± 0.21 x 10^{-3} cm^{-1} and H = -4.68 ± 0.24 x 10^{-5} cm^{-1}.) These computations show that one could reasonably assume that the laser line pumps both the 2_{02}-2_{12} and 3_{03}-3_{13} transitions simultaneously since the Doppler broadening at the flame temperature (vide infra) is about 0.12 cm^{-1}. Since the results in Table 1 predict that the laser line overlaps the former transition much better than the latter, they are qualitatively in good agreement with the intensity distribution of the fluorescence spectrum of Figure 1. For example, in the absorption spectrum of Dressler and Ramsay,[2] the 2_{02}-3_{12} is ~2 times weaker than the 3_{03}-4_{13} transition and the 2_{02}-1_{10} is 3-4 times weaker than the 3_{03}-2_{11} transition. In the fluorescence spectrum of Figure 1, the 2_{02} transitions are much more intense relative to the 3_{03} transitions. In the $P_{Q_1,N}$ branch, all of the lines overlap at our resolution, resulting in a single, strong line. The remaining lines in the other two branches must arise from rotational energy transfer that is very slow compared to electronic quenching by flame molecules since only a few, very weak rotational lines, other than those arising from the two levels directly pumped by the laser, are observed. Although there is one rather strong, unidentified line in this region, little doubt can remain regarding the NH_2 pumping mechanism. Later in this section, evidence corroborating that the unidentified line arises from NH_2 will be given. In addition, the location of the laser line relative to the two pumping lines will be determined more precisely in the next section.

Table 1. Calculated Frequencies of Some Rotational Lines of the $\tilde{A}^2A_1$ $(0,11,0)\Sigma$ - $\tilde{X}^2B_1$ $(0,2,0)$ Transition of NH_2*

Transition	Frequency (cm^{-1})
1_{01}-1_{11}	15450.30
2_{02}-2_{12}	15449.48
3_{03}-3_{13}	15449.30
4_{04}-4_{14}	15450.93
5_{05}-5_{15}	15455.29

*The 6471Å laser line corresponds to an energy of 15449.56 ± 0.12 cm^{-1}.[40]

It was desirable to identify more bands that result from emission of the $\tilde{A}^2A_1$ (0,11,0)Σ level to the ground state levels. Two of these bands are located in the regions of 5910Å and 6580Å. They are the (0,11,0)-(0,1,0) and (0,11,0)-(1,0,0) bands, respectively (see Figures 2 and 3). There are many more unknown lines in these bands, which explains the initial difficulty encountered in attempts to identify similar patterns of the various vibrational bands in the spectrum. However, if these unidentified lines are neglected, the similarity of these bands to the (0,11,0)-(0,0,0) band is easily recognized. Fluorescence from the (0,11,0) excited state to the (0,3,0), (1,1,0) and (0,4,0) ground state levels was also observed. These bands (not shown) were weak, however, and in some cases only the central Q head was observed. In comparison to the other bands, the (0,11,0)-(0,0,0) band is much less complicated. This band has a very high S/N ratio, enabling us to identify even the weakest features, i.e., the 4_{04}-5_{14} and 4_{04}-3_{12} transitions, unambiguously. The weak lines from 1_{01} and 4_{04} indicate that rotational transfer in the flame environment is slow in comparison to electronic quenching.

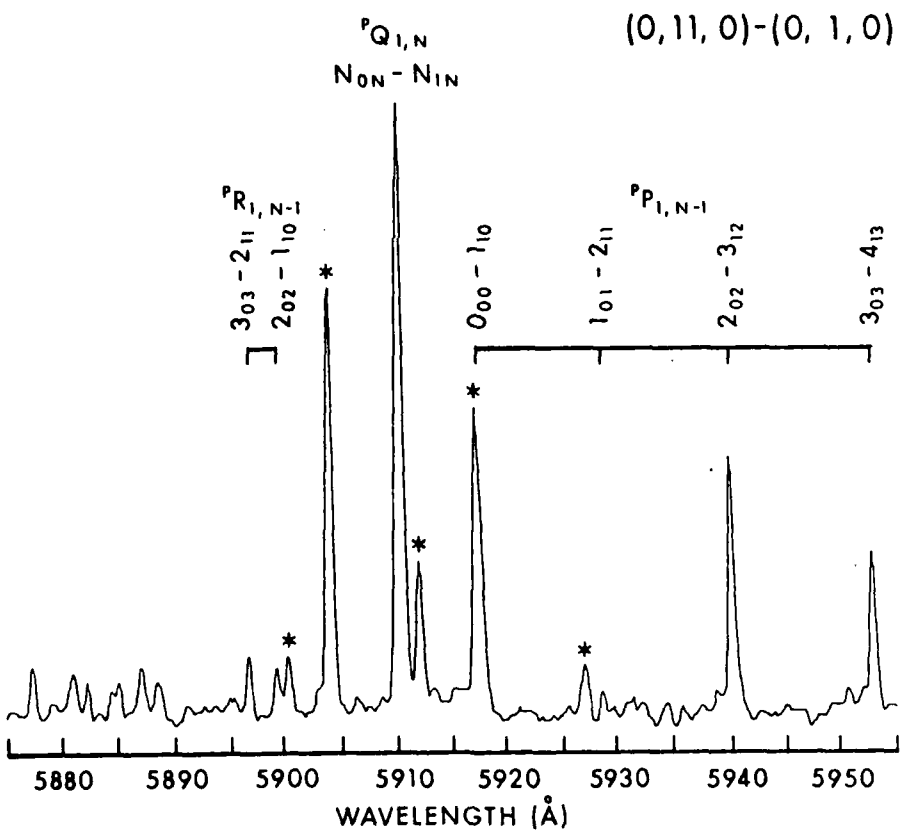

Figure 2. The (0,11,0)-(0,1,0)Σ Band of the $\tilde{A}$-$\tilde{X}$ Transition of NH_2 (as in Figure 1)

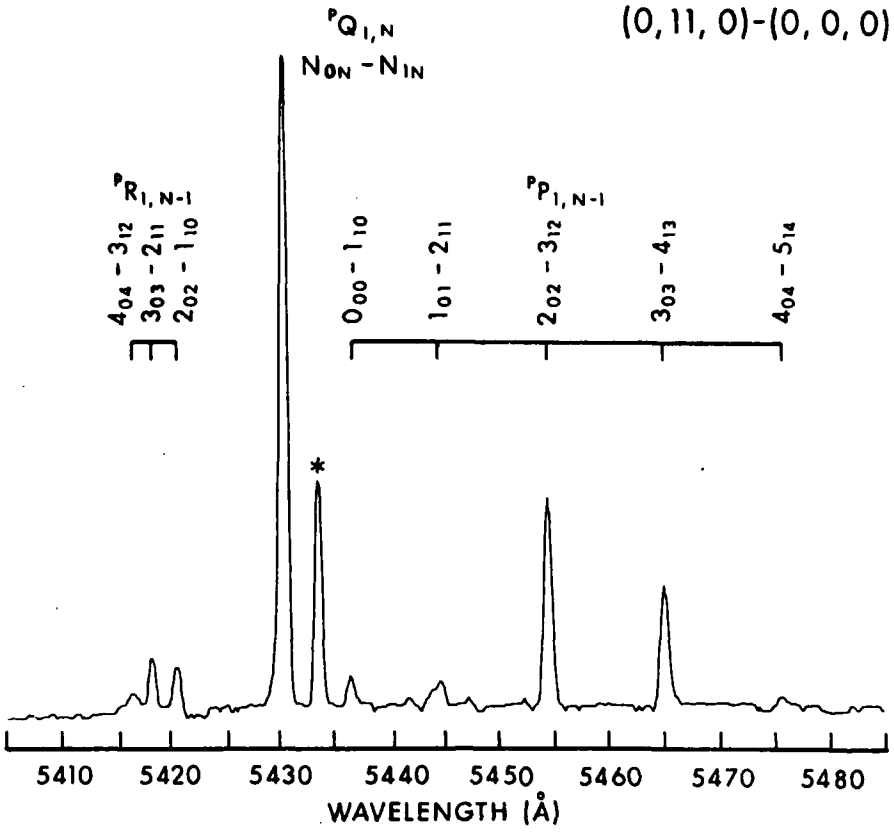

Figure 3. The (0,11,0)-(1,0,0)Σ Band of the $\tilde{A}$-$\tilde{X}$ Transition of NH_2 (as in Figure 1)

To conclude this section, the rest of the spectrum is discussed here. It was previously mentioned that the (0,10,0), (0,9,0), (0,8,0), and (0,7,0) Q heads were identified in the fluorescence spectrum. These probably arise from collisionally induced vibrational energy transfer in the excited state prior to emission, resulting in fluorescence signals of NH_2 over the entire region from 5300Å to ~8000Å where the detection system sensitivity falls off. These bands are weak in comparison to bands from the directly pumped vibrational level. This result indicates that vibrational transfer is small in comparison to electronic quenching, in agreement with the results of Halpern, et al.,[16] who studied NH_2 in the presence of NH_3 and Ar, and of Donnelly, et al.,[17] who studied NH_2 in pure ammonia. Unfortunately, there are many strong and sharp, unidentified lines (see Figures 1-3), most of which lie toward the long wavelength end of the spectrum. Unassigned, poorly understood lines have often been observed in the spectra of NH_2.[2,12,14a,18,21,23,33] Dressler and Ramsay[2] suggested that some of the unidentified lines may belong to bands of other progressions or even to bands of a second electronic transition. Some of these extra lines may be due to perturbations of the upper state by high vibrational levels of the ground state.[18,21] Such perturbations could not be the cause of the unidentified lines shown in Figures 1-3 because, although all

three bands have a common upper vibrational level, none of the unidentified lines appears in the same position in all three bands. There are at least three possible explanations for these lines: (1) More NH_2 transitions than those already identified are pumped by the laser. Such unknown pumping transitions could easily arise from an excitation of a band in which both v_1' and v_1'' and/or v_3' and v_3'' are nonzero. This possibility cannot be ruled out because nonzero v_1'' and v_3'' states have appreciable populations at the flame temperature. Transitions such as described have not received much, if any, study. (2) The unidentified lines are due to Fermi type interactions amongst the ground state vibrational levels. The appearance of more of the unidentified lines towards the red end of the spectrum would then appear as the logical result of more Fermi resonances being possible as the ground state vibrational energy and, hence, density of vibrational levels, increases. (3) At least one species besides NH_2 is being pumped by the laser and gives rise to the unknown lines. If the unidentified line in the 5430Å region (Figure 1) arises from said species, then this species is confined to the flame front and its density is roughly proportional to that of NH_2. This would have to be the case because spectra taken at several different positions in the flame front show that the intensity of this unidentified line is proportional to that of the other lines in this region which arise from NH_2. The absolute intensity of the NH_2 lines falls rapidly outside the flame front (vide infra). Along these lines, we should mention that in the $CH_4/N_2O/N_2$ flame two separate transitions of CN are known to be excited. One of these pumps to v'=6 in the $A^2\pi$ state. Emission from v'=6 and lower levels populated by vibrational down-transfer dominates the spectrum in the methane flame at wavelengths above 6000Å. (The CN excitations will be the subject of future publications).

B. NH_2 Density in the $H_2/N_2O/N_2$ Flame

A detailed description of the methods of obtaining temperature and relative concentration profiles has been given earlier.[29a] As stated in the experimental section, use of the 25 cm monochromator system allowed for the simultaneous measurement of the entire $(0,11,0)-(0,0,0)\Sigma$ subband of NH_2 along with the spontaneous Raman signal from the anti-Stokes vibrational Q branch of N_2. Plots of these spectra as a function of vertical position in the flame appear in Figure 4. The strong peaks to the left are due to the $(0,11,0)-(0,0,0)\Sigma$ fluorescence of the NH_2, seen at a resolution of about 3Å. The smaller peaks to the right are the antistokes Raman signal of N_2. Observe the Raman signal as one traverses the flame front. In the unburnt gases, the signal starts out as a single band due to the 1←0 vibrational transition of N_2. As one moves toward the burnt gas region, the temperature increases and a second vibrational band from the 2←1 transition may be observed to the right of the 1←0 band. A multiparameter least squares program, similar to that used previously for the Stokes signals,[28a] was used to extract the flame temperature as a function of position from these anti-Stokes signals. The relative intensity from the NH_2 signal, integrated over the band shown in Figure 4, may then readily be used to obtain an accurate relative density profile of NH_2 in the flame. To do this one must make two assumptions. The first is that the quenching rate, Q, for excited NH_2 by the flame molecules is constant as a function of position in the flame. Although the temperature and species concentrations have large gradients in the flame zone, work on OH[41,42] and CH[43] in flames has shown that large variations in Q do not occur for these species. Since it may be shown that the majority of the LIF measurements are

made in a region where the composition is mainly that of burnt gases, this result is perhaps not too surprising and is generally applicable to trace species in flames. The second assumption is that the ground state NH_2 is in thermal equilibrium with the flame gases. Upon making these assumptions one finds that in general the relative density profiles closely follow the LIF intensity profiles[29a] so that the latter may be used without corrections. Figure 4 therefore indicates that the NH_2 density rapidly rises to a maximum and then decays somewhat more slowly as one traverses the flame zone. This is seen in Figure 5 where the integrated NH_2 intensity from the $(0,11,0)-(0,0,0)\Sigma$ band and the temperatures are shown as a function of position in the flame. The adiabatic flame temperature was computed to be 2056 K using the code of Svehla and McBride.[44] Note the agreement of the adiabatic and measured flame temperatures which indicates that there is little heat loss to the burner.

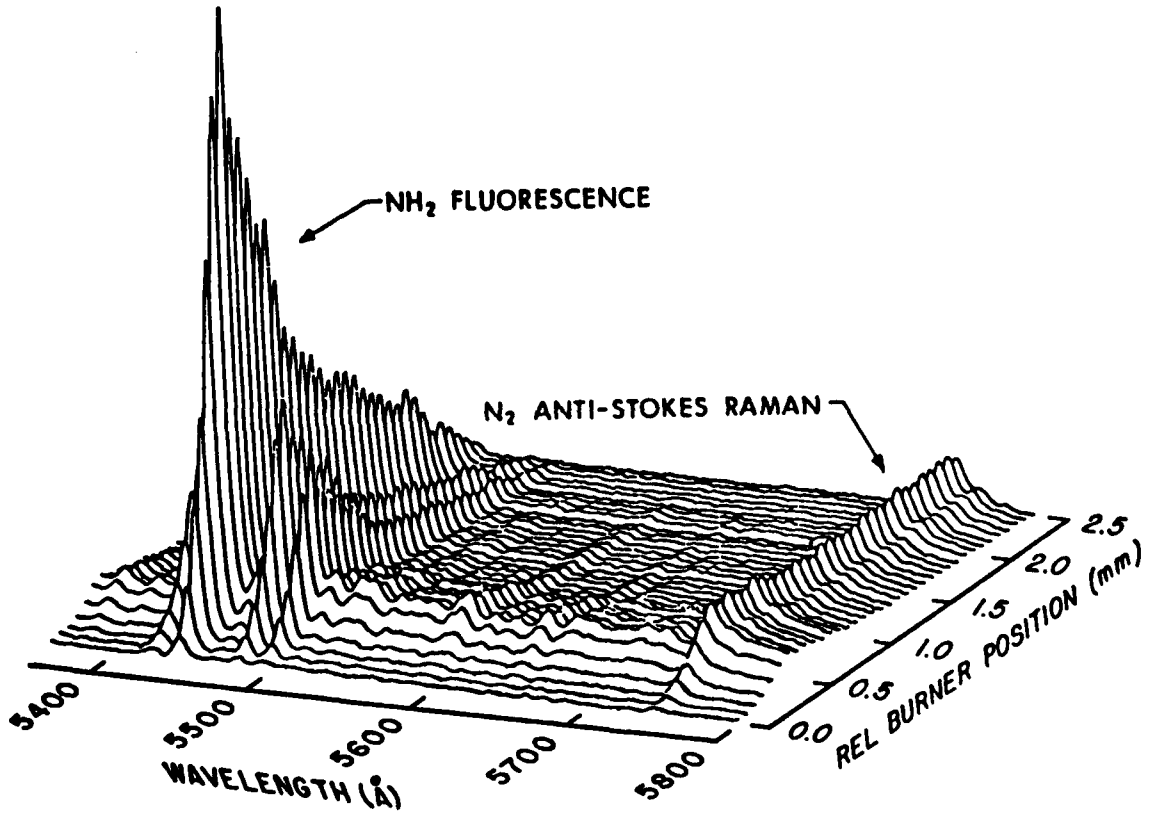

Figure 4. Flame Spectra Taken at Various Heights in $H_2/N_2O/N_2$ Flame

An estimate of the absolute density of the NH_2 requires knowledge of the overlap of the laser line with the molecular transition. The overlap is very difficult to determine in the case of a single transition. This results because the overlap is extremely sensitive to the exact spacing between the laser line and the molecular transition. (A few hundredths of a cm^{-1} can make a large difference - see, for instance, Ref. 29a.) One might at first think that this sensitivity would become even more troublesome when two transitions are simultaneously pumped because of the higher spectral complexity. However, in the present case we have been able to turn this complication to our advantage and determine the relative overlaps of the laser line with the two

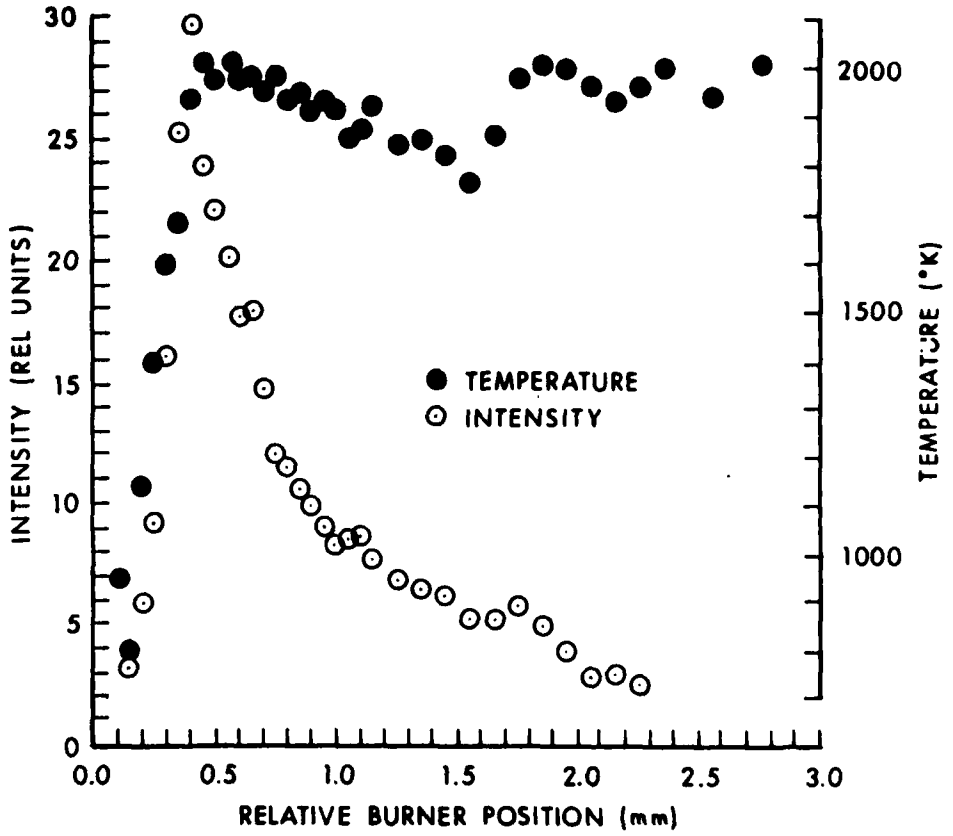

Figure 5. Relative NH_2 Fluorescence Intensity and Temperature as a Function of Position in the $H_2/N_2O/N_2$ Flame. The relative NH_2 density profile is identical to the intensity profile. An estimate of the peak density is given in the text.

pumping transitions. This in turn has allowed the determination of the relative position of the laser line with respect to the two transitions with a precision of ± 0.01 cm^{-1}. The availability of the resolved fluorescence spectrum, Figure 1, allows this determination to be made. We first note from Figure 1 that there is very little rotational transfer to states other than the pumped levels. In addition, recall that experiments of Kroll[13] and of Halpern, et al.,[16] indicate that there will be very little rotational energy transfer between the two pumped levels because the ortho-para transfer is quite slow. We assume that the quenching rate, Q, for the two directly pumped levels is equal. Under these conditions it is readily shown that the relative emission intensity in the two strong $^PP_{1,N}$ branch lines of Figure 1 is given by

$$S_1/S_2 = A_1B_1\sigma_1N_1/A_2B_2\sigma_2N_2 \qquad (1)$$

where S_1 and S_2 are fluorescence signals from the 2_{02}-3_{12} and 3_{03}-4_{13} transitions, respectively. (Note that we have also made the tacit assumption that spin-splitting of the (0,11,0) ← (0,?,0)Σ pumping transition is negligible. This is true for the (0,11,0) - (0,0,0)Σ band (see Ref. 2). However, no measurements are readily available for splittings in the pumped vibrational band.) A_1 and A_2 are the respective Einstein emission coefficients for these transitions. B_1 and B_2 are the Einstein absorption coefficients for 2_{02}-2_{12} and 3_{03}-3_{13} in the (0,11,0)-(0,2,0)Σ band, respectively, and σ_1 and σ_2 are the respective overlaps of the pumping transitions with the laser line. N_1 and N_2 are the densities of 2_{12} and 3_{13} in the (0,2,0) ground state level. Making the assumption that the electronic transition moment is unaffected by changes in N or K_c within a given vibrational band, one finds that the Einstein coefficients are proportional to $S_{N'N''}/(2N'+1)$, where $S_{N'N''}$ is the rotational linestrength, ignoring spin-splitting, for the appropriate transition. It should be noted that Green and Miller[31] using a high resolution laser scan have found that the oscillator strengths of individual lines in a spin-split $^PQ_{1,N}$ doublet from the (0,9,0)-(0,0,0)Σ band are identical. This result is probably not serendipitous. Satellite transitions for which $\Delta J \neq \Delta N$ are very weak even at the lowest N values.[12] When this is the case, one expects to find nearly equal oscillator strengths for the two spin-split lines. Therefore, the assumption that spin-splitting may be ignored in the calculation of main branch linestrengths is justified. The $S_{N'N''}$ were calculated using the direction cosine matrix elements of Cross, et al.,[45] and the eigenvectors resulting from the diagonalization of a Wang transformed asymmetric top Hamiltonian without spin.[46,47] It should be stressed here that the ground and excited state asymmetry parameters, κ, are not assumed to be the same, as in the earlier work,[2,18] but are calculated to be -3.84 and -1, respectively, as determined from the observed spectral parameters.[26] Since the upper state is quasi-linear with Σ character, only matrix elements having K'=0 are possible. For the type-c transitions considered here, nonzero direction cosine matrix elements result when $\Delta K = \pm 1$. Consequently, the only allowed transitions are for K"=1 levels. For Q branch transitions, for which $S_{N'N''}/(2N''+1) = 1/2$ in the limiting symmetric top case, the calculation reduces to the very simple form

$$\frac{S_{N'N''}}{2N''+1} = c''^2_{K=1}/2 \quad , \tag{2}$$

where $c''_{K=1}$ is the mixing coefficient of the K"=1 level. The necessary linestrengths, normalized to 2N'+1, are given in Table 2. The ratio N_1/N_2 is given by the appropriate Boltzmann fraction at the measured flame temperature of ~2000 K. Finally, S_1/S_2 may be obtained from the ratio of the appropriate peak heights in Figure 1. Thus, the value of σ_1/σ_2 is determined. While the relative position of the laser line with respect to the two pumping transitions is not known very precisely from prior measurements (see Table 1), the splitting between the two NH_2 pumping transitions is known. (The problem of relative spacing of the laser line and pump transitions arises because no one has measured the NH_2 and Kr^+ line positions simultaneously. In fact, the relevant NH_2 lines have never been directly observed. In addition, the Kr^+ line position is only known to ± 0.12 cm^{-1}. It is therefore difficult to place the pump line relative to the NH_2 transitions to within better than 0.12 cm^{-1}.) Therefore by making appropriate assumptions about the lineshapes, one may calculate σ_1 and σ_2 as a function of the relative laser line

position. We assumed that the NH_2 transitions are Doppler broadened at the measured flame temperature of ~2000 K (linewidth ~0.12 cm^{-1} FWHM). Note that previous measurements on OH in a flame at atmospheric pressure[48] and on NH_2 at low pressure[31] indicate that collisional broadening is probably a very small correction. The laser line was assumed to be Doppler broadened at 300 K (linewidth ~0.02 cm^{-1} FWHM). σ_1 and σ_2 were rewritten in terms of a single variable, $\Delta\bar{\nu}$, the spacing between the 2_{02}-2_{12} transition and the laser line. An iterative procedure was then used with Eq. (1) and the observed intensity ratio to obtain $\Delta\bar{\nu}$. The results were surprisingly insensitive to the laser linewidth (this is a very important point because the laser line could easily be power broadened; a range from 0.01 - 0.10 cm^{-1} was tried), temperature within its error limits of ~±50 K, the ratio S_1/S_2 within its error limits and the splitting of 0.18 cm^{-1} between the 2_{02}-2_{12} and 3_{03}-3_{13} transitions (see Table 1). The latter was varied from 0.16 - 0.20 cm^{-1}. (This range was chosen based on our estimated uncertainty of ±0.02 cm^{-1} in the calculated splitting of the lines.) The laser line position was thus determined to be between the two pumping transitions, 0.06 ± 0.01 cm^{-1} from the 2_{02}-2_{12} transition. In addition, relative values of the pumping rate, $B_1N_1\sigma_1 + B_2N_2\sigma_2$, were also determined. Error limits on the input data were such that these relative values only varied by ±15% from the optimum value.

Table 2. Linestrengths for the Overlap Calculations

Transition	$S_{N'N''}/(2N'+1)$
Absorption [(0,11,0) ← (0,2,0)]	
2_{02}-2_{12}	0.5000
3_{03}-3_{13}	0.4979
Emission [(0,11,0) → (0,0,0)]	
2_{02}-3_{12}	0.3959
3_{03}-4_{13}	0.3403

Having knowledge of the relative line positions and the overlaps of the two pumping transitions with the laser line, we proceeded to calculate an estimate of the absolute density using the methods discussed in detail in Ref. 29a. Franck-Condon factors (FCFs) for the appropriate vibrational bands were obtained from the work of Jungen, Hallin, and Merer.[49] The FCFs were combined with the transition moment[18] (obtained via LIF lifetimes measurements) to obtain Einstein A coefficients for the vibrational bands of interest. The NH_2 partition function was calculated as in Ref. 31. The quenching rate constant used was that obtained by Halpern, et al.,[16] for pure N_2. (It is interesting to note that their rate constant is quite close to the expected hard-sphere collisional rate constant). This yields a quenching rate of 1.47×10^9 sec^{-1} at the flame temperature, assuming the quenching cross section does not vary with

temperature. The only major difference in the present determination and that for C_2 and CN[29a] and NCO[30] is that the NH_2 fluorescence intensity was compared to the N_2 anti-Stokes (rather than Stokes) Q-branch signal which was readily available (see Figure 4). The appropriate equation for the anti-Stokes Raman signal is

$$E_{AS} = (P_o/h\nu_\ell)\sigma_\ell(\nu_\ell/\nu_{AS})N_{N_2} L\Omega\varepsilon R \qquad (3)$$

where E_{AS} is the number of anti-Stokes photons detected per unit time, P_o is the laser power, σ_ℓ is the Raman scattering cross section for N_2, ν_ℓ and ν_{as} are the laser and anti-Stokes frequencies, respectively, N_{N_2} is the density of N_2 (known from equilibrium flame calculations), L is the length of the excited region viewed by the collection optics, Ω is the collection optic's solid angle, and ε is the detector efficiency. Finally, R is given by

$$R = \sum_{v=1}^{\infty} G / \sum_{v=0}^{\infty} G \qquad (4)$$

where $G = (v+1)\exp(-E_v/kT)$. Equation (4) accounts for the fact that v=0 is not active in the Raman anti-Stokes branch of N_2. The sums in Eq. (4) were truncated at v=5. The resulting estimated peak density of NH_2 in the flame was 9.3×10^{13} cm^{-3}.

Before leaving this section, two points should be made concerning the estimated peak density. The first is that if the quenching rate were very well known, the error limits for the absolute density would only be about ±20%. The major source of this error is in the calculation of overlaps of the laser line with the molecular transitions. However, our assumed quenching rate estimated using the cross sections of Halpern, et al.,[16] is probably only good to within a factor of about 2-3. This is the case because all of the surrounding gas was assumed to be N_2, while in fact only about 60% of it is, the rest being composed mostly of nearly equal parts of H_2 and H_2O. (The combined concentration of other species is expected to be less than 10% at the point where the measurements were performed and is not considered further.) Also, the quenching rate of NH_2 by N_2 was measured at about 298 K. The measured flame temperature was much higher than this. There is no guarantee that the quenching cross section is constant vs. temperature as was assumed. In addition, the quenching measurement of Halpern, et al., was performed for a different excited state vibrational level than was pumped in the present work. Halpern, et al., have, however, shown that the quenching rate is constant vs. vibrational level pumped for NH_3 quencher. Since the measured density is proportional to Q, error limits in the density are also a factor of 2-3. Of course, the relative density profile of Figure 5 has much higher precision than this. The value of Q used is given so that the absolute density may be corrected if better estimates of Q become available. The second point we would like to make is that the Einstein coefficients computed for NH_2 are believed to be quite accurate. To investigate this further, measured and calculated oscillator strengths for two transitions are compared here. In rich NH_3/O_2 flames, previous work has shown that the reactions

$$NH_2 + OH = NH + H_2O \qquad (5)$$

and

$$NH_3 + OH = NH_2 + H_2O \qquad (6)$$

are rapidly equilibrated.[32,50,51] If one knows thermodynamic data precisely enough, equilibrium constants for (5) and (6) may be calculated. Thus, by doing appropriate absorption measurements on reactants involved in (5) and (6), one can determine oscillator strengths for the NH_2 transitions. Chou, Dean, and Stern[32a] thus found an oscillator strength of $2.04\pm0.44\times10^{-4}$ for the $^{P}Q_{1,N}$ 7 transition in the (0,9,0)-(0,0,0)Σ band. However, using different data they later[32c] found this oscillator strength to be $\sim6.4\times10^{-5}$. The $^{R}Q_{1,N}$ 4 transition in the (0,12,0)-(0,0,0)Σ band similarly has had two very different oscillator strengths reported. Nadler, Wang, and Kaskan[50] found a value of $\sim4\times10^{-4}$ for this oscillator strength. Fisher[51] later performed measurements under very similar conditions and found a value of $2.4\pm0.8\times10^{-4}$ for this quantity. He attributed his different result primarily to the use of newer thermochemical data. Calculated oscillator strengths for these two transitions were obtained in the following manner. Einstein A coefficients for the (0,9,0)-(0,0,0)Σ and (0,12,0)-(0,0,0)π bands were calculated using the transition moment[18] and calculated FCFs.[49] $S_{N'N''}/(2N'+1)$ values of 0.451 and 0.709 were then calculated for the $^{P}Q_{1,N}7$ line in the former band and the $^{R}Q_{0,N}4$ line in the latter band, respectively. One finds these values lead to Einstein A coefficients of $3.65 \pm 0.37 \times 10^{4}$ sec^{-1} and $7.09 \pm 0.71 \times 10^{4}$ sec^{-1} and oscillator strengths of $1.96 \pm 0.20 \times 10^{-4}$ and $2.84 \pm 0.28 \times 10^{-4}$, respectively. Error limits here arise from the error limits reported in the fit of experimental data to yield the transition moment.[18] The fact that the two calculated oscillator strengths are nearly identical is coincidental. The measured oscillator strengths are of the correct order of magnitude to agree with our calculated values. However, the measured oscillator strengths are quite sensitive to the exact choice of thermochemical data used, in particular the heats of formation of NH and NH_2. It would appear that our calculated oscillator strengths are presently the best choices for these quantities and are, in fact, much more accurate than the measured values. We believe this to be the case because the FCF calculations of Jungen, et al.,[49] coupled with the ab initio transition moment of Peyerimhoff and Buenker[52] yield lifetimes of various vibrational levels of the A state of NH_2 in excellent agreement with experiment. (A calculation of the $\tilde{A}$-$\tilde{X}$ transition moment in Ref. 53 results in a value somewhat different from that in Refs. 18 and 52, probably because no configuration interaction was included. These calculations were only carried out at the MCSCF level because the primary interest was in mapping out the NH_2 potentials, not in determining the $\tilde{A}$-$\tilde{X}$ transition moment.) In addition, the transition moment from the fit to experimental data[18] is in very good agreement with the ab initio result. Finally, ab initio calculations of the relative vibrational band intensities[54] are in reasonable agreement with calculated FCFs from the semiempirical fitting procedure.[49] A review of the NH and NH_2 heats of formation and the NH_2 oscillator strengths calculated from the flame measurements is currently underway.[55]

IV. CONCLUSIONS

Laser excitation of NH_2 using the 6471Å line of a Kr^+ laser has been observed. This line simultaneously pumps two rotational transitions in the (0,11,0)-(0,2,0)Σ vibrational hot band. The fluorescence spectrum was used to extract a precise measurement of the relative placement of the laser line and the two pumping transitions. In addition, a precise relative density profile of NH_2 in an $H_2/N_2O/N_2$ flame was obtained. An estimate of the peak density was also determined.

Use of LIF to determine absolute flame radical densities has historically been hampered by a lack of knowledge of the quenching rates of the excited species by flame molecules.[56] Several methods for circumventing this problem, including measurement of Q in low pressure flames, were reviewed in Ref. 56. Recently Bechtel and coworkers[57] have shown that Q may be directly measured in atmospheric pressure flames, via fluorescence lifetime measurements, using an ion laser pumped, picosecond, doubled dye laser system. Our observation of coincidences of ion laser lines with transitions of several radicals suggests that the direct measurement of Q in atmospheric pressure flames might be accomplished by simply using a picosecond ion laser to pump these radicals. The absolute radical density could then be obtained from (amongst other more well-known parameters) the LIF signal strength, the measured value of Q, and a knowledge of the overlap of the laser line with the molecular transition. Of course, the latter is known precisely only for the NH_2 radical from the present work. Measurement of this parameter could be difficult for other radicals. However, it should be pointed out that OH, which is very important chemically in combustion systems, is one of the radicals which may be pumped with the Kr^+ laser.[28a] Therefore, some research in this direction should prove to be valuable.

ACKNOWLEDGEMENTS

Koon Wong would like to express his gratitude to the Ballistic Research Laboratory and to the National Research Council for a postdoctoral fellowship. The authors thank Dr. D.A. Ramsay for sending the original data for Ref. 13 and Dr. M. Vervloet for sending information concerning the (0,2,0) and (0,3,0) $\tilde{X}^2B_1$ levels of NH_2.

REFERENCES

1. H.C. Dibbits, "I. Ueber die Spectra der Flammen Einiger Gase," Pogg. Ann., Vol. 122, p. 497, 1864.

2. K. Dressler and D.A. Ramsey, "The Electronic Absorption Spectra of NH_2 and ND_2," Phil. Trans. R. Soc. London Ser., Vol. A251, p. 553, 1959.

3. R.N. Dixon, "The Renner Effect in a Nearly Linear Molecule, with Application to NH_2," Mol. Phys., Vol. 9, p. 357, 1965.

4. J.A. Logan, M.J. Prather, S.C. Wofsy, and M.B. McElroy, "Troposheric Chemistry: A Global Perspective," J. Geophys. Res., Vol. 86, p. 7210, 1981.

5. A.G. Gaydon and H.G. Wolfhard, Flames, Chapman and Hall, London, 1979.

6. W.C. Gardiner, Jr. and D.B. Olson, "Chemical Kinetics of High Temperature Combustion," Ann. Rev. Phys. Chem., Vol. 31, p. 377, 1980.

7. J.A. Silver, "Determination of Kinetic Parameters of Combustion Processes Using Optical Detection Techniques," Opt. Eng., Vol. 20, p. 540, 1981.

8a. M. Gehring, K. Hoyermann, H. Schacke, and J. Wolfrum, "Direct Studies of Some Elementary Steps for the Formation and Destruction of Nitric Oxide in the H-N-O System," 14th Symposium (International) on Combustion, The Combustion Institute, Pittsburgh, p. 99, 1973.

b. P. Andresen, A. Jacobs, C. Kleinermanns, and J. Wolfrum, "Direct Investigations of the NH_2 + NO Reaction by Laser Photolysis at Different Temperatures," 19th Symposium (International) on Combustion, The Combustion Institute, Pittsburgh, p. 11, 1982.

9. A.M. Dean, J.E. Hardy, and R.K. Lyon, "Kinetics and Mechanism of NH_3 Oxidation," 19th Symposium (International) on Combustion, The Combustion Institute, Pittsburgh, p. 97, 1982.

10. G. Herzberg and D.A. Ramsay, "Absorption Spectrum of Free NH_2 Radicals," J. Chem. Phys., Vol. 20, p. 347, 1952.

11. D.A. Ramsay, "The Absorption Spectra of Free NH and NH_2 Radicals Produced by the Flash Photolysis of Hydrazine," J. Phys. Chem., Vol. 57, p. 415, 1953.

12. J.W.C. Johns, D.A. Ramsay, and S.C. Ross, "The $\tilde{A}^2A_1$-$\tilde{X}^2B_1$ Absorption Spectrum of NH_2 Between 6250 and 9500Å," Can. J. Phys., Vol. 54, p. 1804, 1976.

13. M. Kroll, "The Fluorescence Spectrum of NH_2 Excited by a CW Dye Laser," J. Chem. Phys., Vol. 63, p. 4808, 1975.

14a. M. Vervloet and M.F. Merienne-Lafore, "New Vibronic Levels of NH_2 Excited by a Blue CW Dye Laser," J. Chem. Phys., Vol. 69, p. 1257, 1978.

b. M. Vervloet and M.F. Merienne-Lafore, "Constantes Moleculaires de (100) $\tilde{X}^2B_1$ de NH_2: Observation et Estimation de la Vibration ν_3," Can. J. Phys., Vol. 60, p. 49, 1982.

15. M. Vervloet, M.F. Merienne-Lafore, and D.A. Ramsay, "Molecular Constants for the 010 Level of the $\tilde{X}^2B_1$ Ground State of NH_2," Chem. Phys. Lett., Vol. 57, p. 5, 1978.

16. J.B. Halpern, G. Hancock, M. Lenzi, and K.H. Welge, "Laser Induced Fluorescence from NH_2 ($^2A_1$). State Selected Radiative Lifetimes and Collisional De-Excitation Rates," J. Chem. Phys., Vol. 63, p. 4808, 1975.

17. V.M. Donnelly, A.P. Baranovski, and J.R. McDonald, "Excited State Dynamics and Bimolecular Quenching Processes for NH_2 ($\tilde{A}^2A_1$)," Chem. Phys., Vol. 43, p. 283, 1979.

18. S. Mayama, S. Hiraoka, and K. Obi, "Laser Induced Fluorescence of NH_2 ($\tilde{A}^2A_1$) in the Supersonic Free Jet," J. Chem. Phys., Vol. 80, p. 7, 1984.

19. T.X. Xiang, L.M. Torres, and W.A. Guillory, "State-Selected Reaction and Relaxation of NH_2 [$\tilde{X}^2B_1$ $(0,\nu_2,0)$] Radicals and NO_2," J. Chem. Phys., Vol. 83, p. 1623, 1985.

20. D.E. Milligan and M.E. Jacox, "Matrix-Isolation Infrared Spectrum of the Free Radical NH_2," J. Chem. Phys., Vol. 43, p. 4487, 1965.

21. G.W. Hills, C.R. Brazier, J.M. Brown, J.M. Cook, and R.F. Curl, Jr., "Microwave Optical Double Resonance Spectrum of NH_2. VII. Hyperfine Coupling Constants (^{14}N and ^1H) in Σ (0,9,0) and π (0,10,0) of $\tilde{A}^2A_1$," J. Chem. Phys., Vol. 76, p. 240, 1982, and references therein.

22. T. Amano, P.F. Bernath, and A.R.W. McKellar, "Direct Observation of the ν_1 and ν_3 Fundamental Bands of NH_2 by Difference Frequency Laser Spectroscopy," J. Mol. Spectrosc., Vol. 94, p. 100, 1982.

23. T. Amano, K. Kawaguchi, M. Kakimoto, S. Saito, and E. Hirota, "Infrared-Optical Double Resonance Spectroscopy of the NH_2 Radical," J. Chem. Phys., Vol. 77, p. 159, 1982.

24. T. Dreier and J. Wolfrum, "Detection of Free NH_2 ($\tilde{X}^2B_1$) Radicals by CARS Spectroscopy," Appl. Phys., Vol. B33, p. 213, 1984.

25. F.W. Birss, D.A. Ramsay, S.C. Ross, and C. Zauli, "Molecular Constants for the Ground State of NH_2," J. Mol. Spectrosc., Vol. 78, p. 344, 1979.

26. F.W. Birss, M.F. Merienne-Lafore, D.A. Ramsay, and M. Vervloet, "The 020 Level in the Ground State of NH_2," J. Mol. Spectrosc., Vol. 85, p. 493, 1981.

27. D.R. Crosley, ed., Laser Probes for Combustion Chemistry, ACS Symposium Series 134, American Chemical Society, Washington, DC, 1980.

28a. J.A. Vanderhoff, W.R. Anderson, A.J. Kotlar, and R.A. Beyer, "Raman and Fluorescence Spectroscopy in a Methane-Nitrous Oxide Laminar Flame," 20th Symposium (International) on Combustion, The Combustion Institute, Pittsburgh, PA, p. 1299, 1984.

b. J.A. Vanderhoff, S.W. Bunte, A.J. Kotlar, and R.A. Beyer, "Temperature and Concentration Profiles in Hydrogen-Nitrous Oxide Flames," to appear in Combustion and Flame.

29a. J.A. Vanderhoff, R.A. Beyer, A.J. Kotlar, and W.R. Anderson, "Ar^+ Laser-Excited Fluorescence of C_2 and CN Produced in a Flame," Combustion and Flame, Vol. 49, p. 197, 1983.

b. J.A. Vanderhoff, R.A. Beyer, A.J. Kotlar, and W.R. Anderson, "Kr^+ and Ar^+ Laser-Excited Fluorescence of CN in a Flame," Appl. Opt., Vol. 22, p. 1976, 1983.

30a. W.R. Anderson, J.A. Vanderhoff, A.J. Kotlar, M.A. DeWilde, and R.A. Beyer, "Intracavity Laser Excitation of NCO Fluorescence in an Atmospheric Pressure Flame," J. Chem. Phys., Vol. 77, p. 1677, 1982.

b. K.N. Wong, W.R. Anderson, A.J. Kotlar, and J.A. Vanderhoff, "Investigation of Several Low-Lying Levels of $X^2\pi$ NCO Using Argon Laser Excited Fluorescence," J. Chem. Phys., Vol. 81, p. 2970, 1984.

31. R.M. Green and J.A. Miller, "The Measurement of Relative Concentration Profiles of NH_2 Using Laser Absorption Spectroscopy," J. Quant. Spectrosc. Radiat. Transfer, Vol. 26, p. 313, 1981.

32a. M.S. Chou, A.M. Dean, and D. Stern, "Laser Absorption Measurements on OH, NH, and NH_2 in NH_3/O_2 Flames: Determination of an Oscillator Strength for NH_2," J. Chem. Phys., Vol. 76, p. 5334, 1982.

b. A.M. Dean, M.S. Chou, and D. Stern, "Nitrogen Chemistry in Flames: Observations and Detailed Kinetic Modeling," in The Chemistry of Combustion Processes, T.M. Sloane, ed., ACS Symposium Series 249, American Chemical Society, Washington, DC, p. 71, 1984.

c. A.M. Dean, M.S. Chou, and D. Stern, "Kinetics of Rich Ammonia Flames," Int. J. Chem. Kin., Vol. 16, p. 633, 1984.

33. R.A. Copeland, D.R. Crosley, and G.P. Smith, "Laser-Induced Fluorescence Spectroscopy of NCO and NH_2 in Atmospheric Pressure Flames," 20th Symposium (International) on Combustion, The Combustion Institute, Pittsburgh, PA, p. 1195, 1984.

34a. R.A. Beyer, "Molecular Beam Sampling Mass Spectrometry of High Heating Rate Pyrolysis: Description of Data Acquisition System and Pyrolysis of HMX in a Polyurethane Binder," BRL Technical Report ARBRL-TR-02816, March 1978, AD# A054328.

b. C.U. Morgan and R.A. Beyer, "ESR and IR Spectroscopic Studies of HMX and RDX Thermal Decomposition," 15th JANNAF Combustion Meeting, Newport, RI, September 1978.

35. R.A. Fifer, "Chemistry of Nitrate Ester and Nitramine Propellants," in Progress in Aeronautics and Astronautics, Vol. 90: Fundamentals of Solid Propellant Combustion, K.K. Kuo and M. Summerfield, eds., American Institute of Aeronautics and Astronautics, Inc., New York, 1984.

36. R.A. Beyer and M.A. DeWilde, "Simple Burner for Laser Probing of Flames," Rev. Sci. Instrum., Vol. 53, p. 103, 1982.

37. G. Herzberg, Molecular Spectra and Molecular Structure. I. Spectra of Diatomic Molecules, Van Nostrand-Reinhold, New York, 1950.

38. J.A. Vanderhoff, R.A. Beyer, and A.J. Kotlar, "Laser Spectroscopy of Flames: Temperature and Concentrations in CH_4/N_2O Flames," BRL Report No. ARBRL-TR-02388, January 1982.

39. J.A. Vanderhoff, unpublished results.

40. G.R. Harrison, Massachusetts Institute of Technology Wavelength Tables, The MIT Press, Cambridge, MA, 1969.

41. M.J. Cotterau and D. Stepowski, "Laser-Induced Fluorescence Spectroscopy Applied to the Hydroxyl Radical in Flames," in Laser Probes for Combustion Chemistry, p. 131, 1980.

42. J.H. Bechtel and R.E. Teets, "Hydroxyl and Its Concentration Profile in Methane-Air Flames," Appl. Opt., Vol. 18, p. 4138, 1979.

43. R.J. Cattolica, D. Stepowski, D. Puechberty and M. Cottereau, "Laser Fluorescence Measurements of the CH Radical in a Low Pressure Flame," J. Quant. Spectrosc. Radiat. Transfer, Vol. 32, p. 363, 1984.

44. R.A. Svehla and B.J. McBride, "Fortran IV Computer Program for Calculation of Thermodynamic and Transport Properties of Complex Chemical Systems," NASA TN D-7056, 1973.

45. P.C. Cross, R.M. Hainer, and G.W. King, "The Assymetric Rotor. II. Calculation of Dipole Intensities and Line Classification," J. Chem. Phys., Vol. 12, p. 210, 1944.

46. J.K.G. Watson, "Determination of Centrifugal Distortion Coefficients of Assymmetric-Top Molecules," J. Chem. Phys., Vol. 46, p. 1935, 1967.

47. C. Camy-Peyret and J.M. Flaud, "Line Positions and Intensities in the ν_2 Band of $H_2{}^{16}O$," Mol. Phys., Vol. 32, p. 523, 1976.

48. R.J. Mainiero and M. Vanpee, "The OH Collision Broadening Parameter in the 2900°K H_2-NO Flame," J. Quant. Spectrosc. Radiat. Transfer, Vol. 23, p. 303, 1980.

49. C. Jungen, K.E.J. Hallin, and A.J. Merer, "Orbital Angular Momentum in Triatomic Molecules. II. Vibrational and K-Type Rotational Structure, and Intensity Factors in the $\tilde{A}^2A_1$-$\tilde{X}^2B_1$ Transitions of NH_2 and H_2O^+," Mol. Phys., Vol. 40, p. 25, 1980.

50. M.P. Nadler, V.K. Wang, and W.E. Kaskan, "The Decay of Radicals in Ammonia-Oxygen-Nitrogen Flames," J. Phys. Chem., Vol. 74, p. 917, 1970.

51. C.J. Fisher, "A Study of Rich Ammonia/Oxygen/Nitrogen Flames," Combustion and Flame, Vol. 30, p. 143, 1977.

52. S.D. Peyerimhoff and R.J. Buenker, "Theoretical Study of the $\tilde{X}^2B_1$, $\tilde{A}^2A_1$, $^2B_2$ Valence Shell and the First π_u ^{2}3s-Type Doublet and Quartet Rydberg States of NH_2," Can. J. Chem., Vol. 57, p. 3182, 1979.

53. R.P. Saxon, B.H. Lengsfield, III, and B. Liu, "Theoretical Study of NH_2: Potential Curves, Transition Moments, and Photodissociation Cross Sections," J. Chem. Phys., Vol. 78, p. 312, 1983; also B.H. Lengsfield, III, private communication.

54. R.J. Buenker, M. Peric, S.D. Peyerimhoff, and R. Marian, "Ab Initio Treatment of the Renner-Teller Effect for the $\tilde{X}^2B_1$ and $\tilde{A}^2A_1$ Electronic States of NH_2," Mol. Phys., Vol. 43, p. 987, 1981.

55. W.R. Anderson, to be published.

56. D.R. Crosley, "Collisional Effects on Laser Induced Fluorescence Flame Measurements," Opt. Eng., Vol. 20, p. 511, 1981.

57. N.S. Bergano, P.A. Jaanimagi, M.M. Salour, and J.H. Bechtel, "Picosecond Laser Spectroscopy Measurement of Hydroxyl Fluorescence Lifetime in Flames," Opt. Lett., Vol. 8, p. 443, 1983.

DISTRIBUTION LIST

No. Of Copies	Organization
12	Administrator Defense Technical Info Center ATTN: DTIC-FDAC Cameron Station, Bldg. 5 Alexandria, VA 22304-6145
1	HQ DA DAMA-ART-M Washington, DC 20310
1	Commander US Army Materiel Command ATTN: AMCDRA-ST 5001 Eisenhower Avenue Alexandria, VA 22333-0001
10	C.I.A. *OIR/DB/Standard* GE47 HQ Washington, DC 20505
1	Commander US Army ARDEC ATTN: SMCAR-MSI Dover, NJ 07801-5001
1	Commander US Army ARDEC ATTN: SMCAR-TDC Dover, NJ 07801
1	Commander US AMCCOM ARDEC CCAC Benet Weapons Laboratory ATTN: SMCAR-CCB-TL Watervliet, NY 12189-4050
1	US Army Armament, Munitions and Chemical Command ATTN: AMSMC-IMP-L Rock Island, IL 61299-7300
1	Commander US Army Aviation Systems Command ATTN: AMSAV-ES 4300 Goodfellow Blvd. St. Louis, MO 63120-1798
1	Director US Army Aviation Research and Technology Activity Ames Research Center Moffett Field, CA 94035-1099
4	Commander US Army Research Office ATTN: R. Ghirardelli D. Mann R. Singleton R. Shaw P.O. Box 12211 Research Triangle Park, NC 27709-2211
1	Commander US Army Communications - Electronics Command ATTN: AMSEL-ED Fort Monmouth, NJ 07703
1	Commander CECOM R&D Technical Library ATTN: AMSEL-IM-L, Reports Section B.2700 Fort Monmouth, NJ 07703-5000
2	Commander Armament R&D Center US Army AMCCOM ATTN: SMCAR-LCA-G, D.S. Downs J.A. Lannon Dover, NJ 07801
1	Commander Armament R&D Center US Army AMCCOM ATTN: SMCAR-LC-G, L. Harris Dover, NJ 07801
1	Commander Armament R&D Center US Army AMCCOM ATTN: SMCAR-SCA-T, L. Stiefel Dover, NJ 07801

DISTRIBUTION LIST

No. Of Copies	Organization
1	Commander US Army Missile Command Research, Development and Engineering Center ATTN: AMSMI-RD Redstone Arsenal, AL 35898
1	Commander US Army Missile and Space Intelligence Center ATTN: AMSMI-YDL Redstone Arsenal, AL 35898-5000
2	Commander US Army Missile Command ATTN: AMSMI-RK, D.J. Ifshin W. Wharton Redstone Arsenal, AL 35898
1	Commander US Army Missile Command ATTN: AMSMI-RKA, A.R. Maykut Redstone Arsenal, AL 35898-5249
1	Commander US Army Tank Automotive Command ATTN: AMSTA-TSL Warren, MI 48397-5000
1	Director US Army TRADOC Systems Analysis Center ATTN: ATOR-TSL White Sands Missile Range, NM 88002-5502
1	Commandant US Army Infantry School ATTN: ATSH-CD-CS-OR Fort Benning, GA 31905-5400
1	Commander US Army Development and Employment Agency ATTN: MODE-ORO Fort Lewis, WA 98433-5000
1	Office of Naval Research Department of the Navy ATTN: R.S. Miller, Code 432 800 N. Quincy Street Arlington, VA 22217
1	Commander Naval Air Systems Command ATTN: J. Ramnarace, AIR-54111C Washington, DC 20360
2	Commander Naval Ordnance Station ATTN: C. Irish P.L. Stang, Code 515 Indian Head, MD 20640
1	Commander Naval Surface Weapons Center ATTN: J.L. East, Jr., G-23 Dahlgren, VA 22448-5000
2	Commander Naval Surface Weapons Center ATTN: R. Bernecker, R-13 G.B. Wilmot, R-16 Silver Spring, MD 20902-5000
1	Commander Naval Weapons Center ATTN: R.L. Derr, Code 389 China Lake, CA 93555
2	Commander Naval Weapons Center ATTN: Code 3891, T. Boggs K.J. Graham China Lake, CA 93555
5	Commander Naval Research Laboratory ATTN: M.C. Lin J. McDonald E. Oran J. Shnur R.J. Doyle, Code 6110 Washington, DC 20375

DISTRIBUTION LIST

No. Of Copies	Organization
1	Commanding Officer Naval Underwater Systems Center Weapons Dept. ATTN: R.S. Lazar/Code 36301 Newport, RI 02840
1	Superintendent Naval Postgraduate School Dept. of Aeronautics ATTN: D.W. Netzer Monterey, CA 93940
4	AFRPL/DY, Stop 24 ATTN: R. Corley R. Geisler J. Levine D. Weaver Edwards AFB, CA 93523-5000
1	AFRPL/MKPB, Stop 24 ATTN: B. Goshgarian Edwards AFB, CA 93523-5000
1	AFOSR ATTN: J.M. Tishkoff Bolling Air Force Base Washington, DC 20332
1	AFATL/DOIL (Tech Info Center) Eglin AFB, FL 32542-5438
1	Air Force Weapons Laboratory AFWL/SUL ATTN: V. King Kirtland AFB, NM 87117
1	NASA Langley Research Center Langley Station ATTN: G.B. Northam/MS 168 Hampton, VA 23365
4	National Bureau of Standards ATTN: J. Hastie M. Jacox T. Kashiwagi H. Semerjian US Department of Commerce Washington, DC 20234
1	OSD/SDIO/UST ATTN: L.H. Caveny Pentagon Washington, DC 20301-7100
1	Aerojet Solid Propulsion Co. ATTN: P. Micheli Sacramento, CA 95813
1	Applied Combustion Technology, Inc. ATTN: A.M. Varney P.O. Box 17885 Orlando, FL 32860
2	Applied Mechanics Reviews The American Society of Mechanical Engineers ATTN: R.E. White A.B. Wenzel 345 E. 47th Street New York, NY 10017
1	Atlantic Research Corp. ATTN: M.K. King 5390 Cherokee Avenue Alexandria, VA 22314
1	Atlantic Research Corp. ATTN: R.H.W. Waesche 7511 Wellington Road Gainesville, VA 22065
1	AVCO Everett Rsch. Lab. Div. ATTN: D. Stickler 2385 Revere Beach Parkway Everett, MA 02149
1	Battelle Memorial Institute Tactical Technology Center ATTN: J. Huggins 505 King Avenue Columbus, OH 43201
1	Cohen Professional Services ATTN: N.S. Cohen 141 Channing Street Redlands, CA 92373

DISTRIBUTION LIST

No. Of Copies	Organization
1	Exxon Research & Eng. Co. Government Research Lab ATTN: A. Dean P.O. Box 48 Linden, NJ 07036
1	Ford Aerospace and Communications Corp. DIVAD Division Div. Hq., Irvine ATTN: D. Williams Main Street & Ford Road Newport Beach, CA 92663
1	General Applied Science Laboratories, Inc. ATTN: J.I. Erdos 425 Merrick Avenue Westbury, NY 11590
1	General Electric Armament & Electrical Systems ATTN: M.J. Bulman Lakeside Avenue Burlington, VT 05401
1	General Electric Company 2352 Jade Lane Schenectady, NY 12309
1	General Electric Ordnance Systems ATTN: J. Mandzy 100 Plastics Avenue Pittsfield, MA 01203
2	General Motors Rsch Labs Physics Department ATTN: T. Sloan R. Teets Warren, MI 48090
2	Hercules, Inc. Allegany Ballistics Lab. ATTN: R.R. Miller E.A. Yount P.O. Box 210 Cumberland, MD 21501
1	Hercules, Inc. Bacchus Works ATTN: K.P. McCarty P.O. Box 98 Magna, UT 84044
1	Honeywell, Inc. Government and Aerospace Products ATTN: D.E. Broden/ MS MN50-2000 600 2nd Street NE Hopkins, MN 55343
1	IBM Corporation ATTN: A.C. Tam Research Division 5600 Cottle Road San Jose, CA 95193
1	IIT Research Institute ATTN: R.F. Remaly 10 West 35th Street Chicago, IL 60616
2	Director Lawrence Livermore National Laboratory ATTN: C. Westbrook M. Costantino P.O. Box 808 Livermore, CA 94550
1	Lockheed Missiles & Space Co. ATTN: George Lo 3251 Hanover Street Dept. 52-35/B204/2 Palo Alto, CA 94304
1	Los Alamos National Lab ATTN: B. Nichols T7, MS-B284 P.O. Box 1663 Los Alamos, NM 87545
1	National Science Foundation ATTN: A.B. Harvey Washington, DC 20550

DISTRIBUTION LIST

No. Of Copies	Organization
1	Olin Corporation Smokeless Powder Operations ATTN: V. McDonald P.O. Box 222 St. Marks, FL 32355
1	Paul Gough Associates, Inc. ATTN: P.S. Gough 1048 South Street Portsmouth, NH 03801
2	Princeton Combustion Research Laboratories, Inc. ATTN: M. Summerfield N.A. Messina 475 US Highway One Monmouth Junction, NJ 08852
1	Hughes Aircraft Company ATTN: T.E. Ward 8433 Fallbrook Avenue Canoga Park, CA 91303
1	Rockwell International Corp. Rocketdyne Division ATTN: J.E. Flanagan/HB02 6633 Canoga Avenue Canoga Park, CA 91304
4	Sandia National Laboratories Combustion Sciences Dept. ATTN: R. Cattolica S. Johnston P. Mattern D. Stephenson Livermore, CA 94550
1	Science Applications, Inc. ATTN: R.B. Edelman 23146 Cumorah Crest Woodland Hills, CA 91364
1	Science Applications, Inc. ATTN: H.S. Pergament 1100 State Road, Bldg. N Princeton, NJ 08540
3	SRI International ATTN: G. Smith D. Crosley D. Golden 333 Ravenswood Avenue Menlo Park, CA 94025
1	Stevens Institute of Tech. Davidson Laboratory ATTN: R. McAlevy, III Hoboken, NJ 07030
1	Textron, Inc. Bell Aerospace Co. Division ATTN: T.M. Ferger P.O. Box 1 Buffalo, NY 14240
1	Thiokol Corporation Elkton Division ATTN: W.N. Brundige P.O. Box 241 Elkton, MD 21921
1	Thiokol Corporation Huntsville Division ATTN: R. Glick Huntsville, AL 35807
3	Thiokol Corporation Wasatch Division ATTN: S.J. Bennett P.O. Box 524 Brigham City, UT 84302
1	TRW ATTN: M.S. Chou MSR1-1016 1 Parke Redondo Beach, CA 90278
1	United Technologies ATTN: A.C. Eckbreth East Hartford, CT 06108

DISTRIBUTION LIST

No. Of Copies	Organization
3	United Technologies Corp. Chemical Systems Division ATTN: R.S. Brown T.D. Myers (2 copies) P.O. Box 50015 San Jose, CA 95150-0015
2	United Technologies Corp. ATTN: R.S. Brown R.O. McLaren P.O. Box 358 Sunnyvale, CA 94086
1	Universal Propulsion Company ATTN: H.J. McSpadden Black Canyon Stage 1 Box 1140 Phoenix, AZ 85029
1	Veritay Technology, Inc. ATTN: E.B. Fisher 4845 Millersport Highway P.O. Box 305 East Amherst, NY 14051-0305
1	Brigham Young University Dept. of Chemical Engineering ATTN: M.W. Beckstead Provo, UT 84601
1	California Institute of Tech. Jet Propulsion Laboratory ATTN: MS 125/159 4800 Oak Grove Drive Pasadena, CA 91103
1	California Institute of Technology ATTN: F.E.C. Culick/ MC 301-46 204 Karman Lab. Pasadena, CA 91125
1	University of California, Berkeley Mechanical Engineering Dept. ATTN: J. Daily Berkeley, CA 94720
1	University of California Los Alamos Scientific Lab. P.O. Box 1663, Mail Stop B216 Los Alamos, NM 87545
2	University of California, Santa Barbara Quantum Institute ATTN: K. Schofield M. Steinberg Santa Barbara, CA 93106
2	University of Southern California Dept. of Chemistry ATTN: S. Benson C. Wittig Los Angeles, CA 90007
1	Case Western Reserve Univ. Div. of Aerospace Sciences ATTN: J. Tien Cleveland, OH 44135
1	Cornell University Department of Chemistry ATTN: T.A. Cool Baker Laboratory Ithaca, NY 14853
1	Univ. of Dayton Rsch Inst. ATTN: D. Campbell AFRPL/PAP Stop 24 Edwards AFB, CA 93523
1	University of Florida Dept. of Chemistry ATTN: J. Winefordner Gainesville, FL 32611
3	Georgia Institute of Technology School of Aerospace Engineering ATTN: E. Price W.C. Strahle B.T. Zinn Atlanta, GA 30332

DISTRIBUTION LIST

No. Of Copies	Organization
1	University of Illinois Dept. of Mech. Eng. ATTN: H. Krier 144MEB, 1206 W. Green St. Urbana, IL 61801
1	Johns Hopkins University/APL Chemical Propulsion Information Agency ATTN: T.W. Christian Johns Hopkins Road Laurel, MD 20707
1	University of Michigan Gas Dynamics Lab Aerospace Engineering Bldg. ATTN: G.M. Faeth Ann Arbor, MI 48109-2140
1	University of Minnesota Dept. of Mechanical Engineering ATTN: E. Fletcher Minneapolis, MN 55455
3	Pennsylvania State University Applied Research Laboratory ATTN: K.K. Kuo H. Palmer M. Micci University Park, PA 16802
1	Polytechnic Institute of NY Graduate Center ATTN: S. Lederman Route 110 Farmingdale, NY 11735
2	Princeton University Forrestal Campus Library ATTN: K. Brezinsky I. Glassman P.O. Box 710 Princeton, NJ 08540
1	Princeton University MAE Dept. ATTN: F.A. Williams Princeton, NJ 08544
1	Purdue University School of Aeronautics and Astronautics ATTN: J.R. Osborn Grissom Hall West Lafayette, IN 47906
1	Purdue University Department of Chemistry ATTN: E. Grant West Lafayette, IN 47906
2	Purdue University School of Mechanical Engineering ATTN: N.M. Laurendeau S.N.B. Murthy TSPC Chaffee Hall West Lafayette, IN 47906
1	Rensselaer Polytechnic Inst. Dept. of Chemical Engineering ATTN: A. Fontijn Troy, NY 12181
1	Stanford University Dept. of Mechanical Engineering ATTN: R. Hanson Stanford, CA 94305
1	University of Texas Dept. of Chemistry ATTN: W. Gardiner Austin, TX 78712
1	University of Utah Dept. of Chemical Engineering ATTN: G. Flandro Salt Lake City, UT 84112
1	Virginia Polytechnic Institute and State University ATTN: J.A. Schetz Blacksburg, VA 24061

DISTRIBUTION LIST

No. Of Copies	Organization
1	Commandant USAFAS ATTN: ATSF-TSM-CN Fort Sill, OK 73503-5600

Aberdeen Proving Ground

Dir, USAMSAA
ATTN: AMXSY-D
AMXSY-MP, H. Cohen
Cdr, USATECOM
ATTN: AMSTE-SI-F
Cdr, CRDC, AMCCOM
ATTN: SMCCR-RSP-A
SMCCR-MU
SMCCR-SPS-IL

USER EVALUATION SHEET/CHANGE OF ADDRESS

This Laboratory undertakes a continuing effort to improve the quality of the reports it publishes. Your comments/answers to the items/questions below will aid us in our efforts.

1. BRL Report Number _____ Date of Report _____

2. Date Report Received _____

3. Does this report satisfy a need? (Comment on purpose, related project, or other area of interest for which the report will be used.) _____

_____

_____

4. How specifically, is the report being used? (Information source, design data, procedure, source of ideas, etc.) _____

_____

_____

5. Has the information in this report led to any quantitative savings as far as man-hours or dollars saved, operating costs avoided or efficiencies achieved, etc? If so, please elaborate. _____

_____

_____

6. General Comments. What do you think should be changed to improve future reports? (Indicate changes to organization, technical content, format, etc.)

_____

_____

_____

CURRENT ADDRESS

Name _____

Organization _____

Address _____

City, State, Zip _____

7. If indicating a Change of Address or Address Correction, please provide the New or Correct Address in Block 6 above and the Old or Incorrect address below.

OLD ADDRESS

Name _____

Organization _____

Address _____

City, State, Zip _____

(Remove this sheet, fold as indicated, staple or tape closed, and mail.)

FOLD HERE

Director
US Army Ballistic Research Laboratory
ATTN: DRXBR-OD-ST
Aberdeen Proving Ground, MD 21005-5066

NO POSTAGE
NECESSARY
IF MAILED
IN THE
UNITED STATES

OFFICIAL BUSINESS
PENALTY FOR PRIVATE USE, $300

BUSINESS REPLY MAIL
FIRST CLASS PERMIT NO 12062 WASHINGTON, DC
POSTAGE WILL BE PAID BY DEPARTMENT OF THE ARMY

Director
US Army Ballistic Research Laboratory
ATTN: DRXBR-OD-ST
Aberdeen Proving Ground, MD 21005-9989

FOLD HERE